

Chronic atrophic gastritis and intestinal metaplasia induced by high-salt and N-methyl-N'-nitro-N-nitrosoguanidine intake in rats

JING YIN^{1*}, JINYU YI^{1*}, CHUN YANG², BO XU¹, JIANG LIN¹, HONGYI HU¹,
XIAOJUN WU², HAILIAN SHI² and XIAOYAN FEI¹

¹Longhua Hospital, Shanghai University of Traditional Chinese Medicine, Shanghai 200032;

²Shanghai Key Laboratory of Compound Chinese Medicines, Institute of Chinese Materia Medica, Shanghai University of Traditional Chinese Medicine, Shanghai 201203, P.R. China

Received August 22, 2019; Accepted September 15, 2020

DOI: 10.3892/etm.2021.9746

Abstract. The aim of the present study was to induce chronic atrophic gastritis (CAG) with intestinal metaplasia (IM) in rats by administering saturated salt and methyl-N'-nitro-N-nitrosoguanidine (MNNG) via oral gavage. Changes in gastric mucosal blood microcirculation and activation of the cyclo-oxygenase-2 (COX-2)/hypoxia inducible factor-1 α (HIF-1 α)/vascular endothelial growth factor (VEGF) signaling pathway during CAG and IM development were investigated. After administering saturated salt and MNNG for 25 weeks, mild atrophy was detected in the stomach of model rats using hematoxylin and eosin staining. CAG with IM was successfully induced in the gastric mucosa of the model rats after 35 weeks. Gastric mucosal blood flow was decreased in comparison with controls as early as 15 weeks after treatment to induce CAG and the mRNA expression levels of COX-2, HIF-1 α , vascular endothelial growth factor receptor (VEGFR)1 and VEGFR2 were increased in comparison with untreated rats as early as 25 weeks after treatment. HIF-1 α , COX-2 and VEGFR2 expression levels were increased as early as 25 weeks after CAG induction treatment when compared to controls and HIF-1 α , COX-2, VEGFR1 and VEGFR2 expression levels were significantly increased after 35 weeks. These findings indicated that administering saturated salt and MNNG by

gavage for 35 weeks successfully induced CAG and IM in rats. Furthermore, the microcirculation was disturbed before activation of the COX-2/HIF-1 α /VEGF signaling pathway.

Introduction

Gastric cancer (GC) is one of the most common malignant gastrointestinal tumors and the third leading cause of cancer deaths worldwide (1). The majority of reported cases of GC are in East Asia, Eastern Europe and South America, and more than half of GC cases occur in developing countries, with the majority in China (1-3). The global incidence rates of chronic atrophic gastritis (CAG) range from 0-10.9% yearly (4), and it takes several years for chronic gastritis to develop into gastric cancer. Dysplasia and intestinal metaplasia (IM) occur after CAG and are considered premalignant lesions of GC (5). CAG and IM greatly increase the risk of GC, as they promote the development of dysplasia (3). Chronic *Helicobacter pylori* (Hp) infection is one of the most important risk factors for GC development. According to the anatomic site and criteria, GC is divided into cardia GC, which arises 2-5 cm from the gastric mucosa distal to the esophagogastric junction, and non-cardia GC which originates from the gastric mucosa distal to the cardia (6). Hp is thought to cause 65-80% of all gastric cancer cases (3), however, Hp is not a risk factor for cardia GC (1,3,7-9). Environmental factors, such as high dietary salt intake and oncogenic agents such as methyl-N'-nitro-N-nitrosoguanidine (MNNG), are also important risk factors, particularly under Hp infection-free conditions (1,3,5,10). In China, the mean sodium intake is 5,400 mg/day, which is much higher than the World Health Organization's recommended daily intake of 2,000 mg (11). Several meta-analyses have shown that excess dietary salt intake is a health hazard worldwide and is associated with CAG and IM (12-14). Studies conducted in Japan and Korea, where residents tend to have high-salt intakes owing to their dietary habits of eating salt-rich traditional foods such as miso soup, found that high-salt intake was related to an increased risk of CAG and IM (12-17).

Animal models are important for drug screening and for studying GC, CAG and IM. Several animal models of CAG are used, such as rats, mouse or Mongolian gerbil (18,19). Gastric mucosal injuries, due to Hp infection, surgery, ethanol

Correspondence to: Professor Hailian Shi, Shanghai Key Laboratory of Compound Chinese Medicines, Institute of Chinese Materia Medica, Shanghai University of Traditional Chinese Medicine, 1200 Cailun Road, Zhangjiang Hi-Tech Park, Shanghai 201203, P.R. China
E-mail: shihailian2003@163.com

Dr Xiaoyan Fei, Longhua Hospital, Shanghai University of Traditional Chinese Medicine, 725 South Wanping Road, Xuhui, Shanghai 200032, P.R. China
E-mail: fei_xiaoyan2513@163.com

*Contributed equally

Key words: chronic atrophic gastritis, high salt, MNNG, COX-2, HIF-1 α , VEGF, gastric mucosal blood flow

or indomethacin, and oncogenic agents (primarily MNNG) are the main causes of CAG with precancerous lesions (20,21). Several studies have shown that a synergistic interaction between Hp and a high-salt diet accelerates chronic inflammation and GC development in Mongolian gerbils (22,23) and a high-salt intake is also associated with CAG and IM (14). However, animal models of CAG induced by MNNG and saturated NaCl (to simulate high-salt intake) are rare (22,23); thus, developing a model of CAG with IM in rats treated with oncogenic agents and saturated NaCl may be beneficial for future research and development of drugs to treat CAG and IM.

Chronic inflammation plays an important role in GC development and progression. Moreover, high-salt intake and interleukin-17 (IL-17) synergistically induce vascular endothelial growth factor (VEGF)-A expression through nuclear factor of activated T cells 5 (NFAT5)/signal transducers and activators of transcription 3 (STAT3) interaction in breast cancer cells (24). High-salt intake also promotes inflammation in the tumor microenvironment and enhances angiogenesis and VEGF expression (25). A previous study showed that microcirculatory disorders existed in CAG (26). However, whether high-salt intake with MNNG can induce microcirculatory disorders and whether the hypoxia-inducible factor (HIF)-1 α pathway is activated during the pathological process of CAG with IM remains uncertain.

In the present study, a new rat model of CAG with IM was developed by administration of saturated salt and MNNG by gavage. Dynamic changes in the gastric mucosal blood microcirculation and activation of the cyclo-oxygenase-2 (COX-2)/HIF-1 α /VEGF signaling pathway during the development of CAG with IM were investigated.

Materials and methods

Materials. MNNG (95%) and sodium chloride (99.8%) were purchased from Sinopharm Chemical Reagent Co., Ltd. The primary antibody against VEGF receptor (VEGFR)1 (cat. no. ab184784) was purchased from Abcam. The primary antibodies against COX-2 (cat. no. 12282S), VEGFR2 (cat. no. 9698S) and glyceraldehyde-3-phosphate dehydrogenase (GAPDH; cat. no. 5174S) were provided by Cell Signaling Technology, Inc. The primary antibody against HIF-1 α (cat. no. 610958) was supplied by Becton-Dickinson and Company.

Animals. A total of 30 male Wistar rats (160-180 g; 5 weeks old) were obtained from Shanghai Laboratory Animal Center of the Chinese Academy of Science (Shanghai, China), and housed in the Laboratory Animal Center of Shanghai University of Traditional Chinese Medicine (Shanghai, China). All rats were housed under a 12-h light/dark cycle at room temperature (25 \pm 2 $^{\circ}$ C) and humidity (60 \pm 2%) with free access to food and water. All animal experiments were conducted according to protocols approved by the Animal Ethics Committee of Shanghai University of Traditional Chinese Medicine (approval no. SZY201703012). For euthanasia, rats were anesthetized by an intraperitoneal injection of 3% pentobarbital sodium (30 mg/kg body weight), once fully anesthetized, rats were sacrificed by cervical dislocation and verification of death was defined by cessation of breathing and faded eye color.

CAG model induction. Rats were randomly divided into the control group (n=10) and 4 model groups (n=5/group). Model rats were treated with MNNG at 200 mg/kg body weight by oral gavage on days 0 and 14. Saturated NaCl (1 ml per rat) was administered 3 times per week by oral gavage for the first 3 weeks. MNNG (600 μ g/kg) and saturated NaCl (1 ml per rat) were then administered by gavage on alternate days (Fig. 1). From week 5, 1 group of 5 model rats was killed every 10 weeks (at weeks 5, 15, 25 and 35).

Measurement of gastric mucosal blood flow (GMBF). Rats were fasted for 24 h, then anesthetized with 3% pentobarbital sodium (30 mg/kg body weight). After exposing the stomach, a fiber-optic probe for laser Doppler flowmetry (Moor Instruments Ltd.) was placed on the stomach wall of the fundus, gastric body and antrum to measure the blood flow in the stomach. The voltage number was recorded to represent the relative GMBF.

Specimen collection. After measuring the GMBF, anesthetized rats were sacrificed by cervical dislocation. The stomach was then quickly removed, cut along the greater curvature and washed with 0.9% sodium chloride. The antral tissues were then separated into two or three parts. A part was fixed for 24-48 h in 10% formalin at room temperature for hematoxylin and eosin (H&E) and alcian blue-periodic acid-Schiff (AB-PAS) staining. The other two parts were used for western blotting and quantitative PCR analysis and stored at -80 $^{\circ}$ C.

Morphological assay. Tissue specimens were fixed for 24-48 h with 10% formalin at room temperature, processed, embedded in paraffin and cut into 5- μ m sections. All sections were stained with H&E and AB-PAS (12), observed under a light microscope and scored according to the histopathological grading standard. The degrees of atrophy and metaplasia were assessed according to the updated Sydney classification as: 1, absent; 2, mild; 3, moderate; or 4, severe (12).

Western blot analysis. Stomach tissue was homogenized on ice with CellLyticTM MT mammalian tissue lysis reagent (Sigma-Aldrich) containing protease and phosphatase inhibitor cocktails and centrifuged at 13,523 x g for 15 min at 4 $^{\circ}$ C. The supernatant was then collected, and the protein concentration was determined via BCA assay. Next, 30 μ g of protein per sample was loaded and separated by SDS-PAGE (8 for HIF-1 α , VEGFR1 and VEGFR2 or 15% for COX-2, GAPDH), then transferred onto polyvinylidene fluoride (PVDF) membranes by a wet-transfer system (Bio-Rad Laboratories, Inc.). The PVDF membranes were then blocked with 5% bovine serum albumin (BSA; cat. no. G611BA0007; Sangon Biotech Co., Ltd.) in 1X phosphate buffered saline with 0.1% Tween-20 (PBST) for 1 h. PVDF membranes were incubated with primary antibodies (each, 1:1,000) against COX-2, HIF-1 α , VEGFR1, VEGFR2 and GAPDH at 4 $^{\circ}$ C overnight. The membranes were further incubated with goat anti-rabbit horseradish peroxidase-conjugated secondary antibodies (Jackson ImmunoResearch Laboratories, Inc.; cat. no. 111-035-003; 1:1,000) for 1 h at room temperature. Thereafter, the protein bands were visualized using an ECL-prime kit (EMD Millipore; cat. no. WBKLS0500)

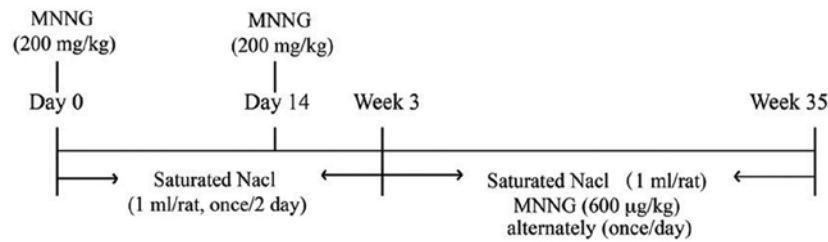


Figure 1. CAG induction protocol in rats. CAG, chronic atrophic gastritis; MNNG, methyl-N¹-nitro-N-nitrosoguanidine.

in a Tanon-5200 (Tanon Science & Technology Co., Ltd.). Quantification of the target proteins was normalized to that of GAPDH within the same sample.

Reverse transcription quantitative PCR (qPCR) analysis. Total RNA was extracted from the stomach tissues using TRIzol[®] reagent (Invitrogen; Thermo Fisher Scientific, Inc.) as per the manufacturer's instructions. cDNA was reverse transcribed from RNA (1 µg) using the RevertAid First Strand cDNA Synthesis kit (cat. no. K1622; Thermo Fisher Scientific, Inc.) according to the manufacturer's protocol. The cDNA (1 µl) was diluted with nuclease-free water 5 times for the qPCR reaction. RT-qPCR was performed using SYBR Premix EX Taq (Roche Diagnostics) on the Quant Studio 6 Flex System (Applied Biosystems; Thermo Fisher Scientific, Inc.) under the following conditions: 95°C for 30 sec, followed by 40 cycles of 95°C for 5 sec, 60°C for 34 sec, 95°C for 15 sec, 60°C for 1 min and 95°C for 15 sec. The target genes were quantified via the $2^{-\Delta\Delta C_q}$ method (27). Table I lists the sequences of primers obtained from Shanghai GeneRay Biotech Co., Ltd. The relative expression of the individual target genes were normalized to that of GAPDH in the same sample.

Statistical analysis. All data are expressed as the mean \pm SEM. Differences between two groups were analyzed using an unpaired Student's t-test. Differences among more than two groups were analyzed using one-way analysis of variance with Dunnett's multiple comparison test. Analyses were performed using GraphPad Prism 6 (GraphPad Software, Inc.). Differences were considered significant at $P < 0.05$.

Results

Atrophic changes in the gastric mucosa. In control rats, stomach glands were arranged neatly and were the same size. After treatment for 5 and 15 weeks, the glands were arranged in order, and the number of glands remained similar (Fig. 2). CAG was detected by HE staining developed in the model rats after 25 weeks. Changes in the glands were much more evident after 35 weeks of treatment than at earlier weeks and compared with the control rats, the glands were reduced in number and visibly disordered. IM, detected by AB-PAS staining, was induced after 35 weeks of induction ($P < 0.01$ vs. control).

IM changes in the gastric mucosa. The AB-PAS staining results showed that, compared with the control rats, glands were decreased in number, but mild IM was not obvious at 25 weeks of treatment (Fig. 3). After 35 weeks of induction,

moderate and severe IM appeared in the antrums of the model rats ($P < 0.001$ vs. control).

GMBF changes at different time points. After 5 weeks of treatment, the GMBF of the fundus, gastric body and antrum did not differ between the control and model rats (Fig. 4). After treatment for 15-35 weeks, the GMBF of the fundus, gastric body and antrum in the model rats was decreased time-dependently, compared with that of the control rats ($P < 0.01$; $P < 0.001$ vs. control).

Activation of the COX-2/HIF-1 α /VEGF pathways at different time points. As early as 25 weeks after treatment, the mRNA expression levels of HIF-1 α ($P < 0.05$ vs. control), COX-2 ($P < 0.01$ vs. control), VEGF ($P < 0.001$ vs. control), VEGFR1 ($P < 0.05$ vs. control) and VEGFR2 ($P < 0.05$ vs. control) were increased compared with those of the control rats. However, the mRNA expression levels of Ang-1 and Ang-2 were not obviously affected (Fig. 5).

Further study demonstrated that the protein expression levels of HIF-1 α ($P < 0.001$ vs. control), COX-2 ($P < 0.05$ vs. control) and VEGFR2 ($P < 0.05$ vs. control), but not VEGFR1 were significantly enhanced in the model rats after 25 weeks compared with those of the control rats (Fig. 6). The protein levels of HIF-1 α ($P < 0.01$ vs. control), COX-2 ($P < 0.05$ vs. control), VEGFR1 ($P < 0.05$ vs. control) and VEGFR2 ($P < 0.05$ vs. control) were obviously upregulated in the model rats after 35 weeks compared with those of the control rats.

Discussion

CAG with IM and dysplasia are the most significant risk factors for GC and considered the two key types of precancerous lesions in GC (1-3). However, the molecular mechanisms of CAG with precancerous lesions are unclear. Suitable animal models that are similar to clinical patients are important for determining the underlying molecular mechanisms of CAG and drug screening and development to treat CAG with precancerous lesions. At present, several methods exist to induce CAG with precancerous lesions in animals. The main methods include Hp infection with or without MNNG (28,29) in Mongolian gerbils, surgery with or without 150 g/l NaCl paste at 50-70°C (30,31), and MNNG with or without the other two or more factors (32-37) (Table II). However, multiple factors, complex operations, long procedure times, high costs and high death rates have resulted in no standard model for CAG with precancerous lesions. Oncogenic agents, such as MNNG, can easily penetrate the pylorus and gastric mucosa

Table I. Primer sequences used in the qPCR analysis.

Genes	Forward primer (5'-3')	Reverse primer (5'-3')
VEGF	CCTCTCCCTACCCCACTTCCT	CACTTTCTCTTTTCTCTGCCTCCAT
VEGFR1	TTGATGGTAGGCTGAGGGATG	AGATGTAAGTCCGAGGATGC
VEGFR2	GAGTTGGTGGAGCATTGGGAA	ATACAGGAAACAGGTGAGGTAGGCA
HIF-1 α	CCCATTCCCTCATCCATCAAACATT	CTTCTGGCTCATAACCCATCAACTC
COX-2	TGAAATATCAGGTCATCGGTGGAG	CATACATCATCAGACCCGGCAC
Ang-1	TTGGTACTCGTCAGACATTTCATC	TCTTCTTCTCTTTTTCCTCCCTTTA
Ang-2	AAGTCAACGCTGCCATCTTCC	GACCTTCCCCAACTCCACAGA
GAPDH	TCTCTGCTCCTCCCTGTTCT	ACACCGACCTTCACCATCT

COX-2, cyclooxygenase-2; HIF, hypoxia inducible factor; VEGFR, vascular endothelial growth factor receptor; Ang, angiotensin.

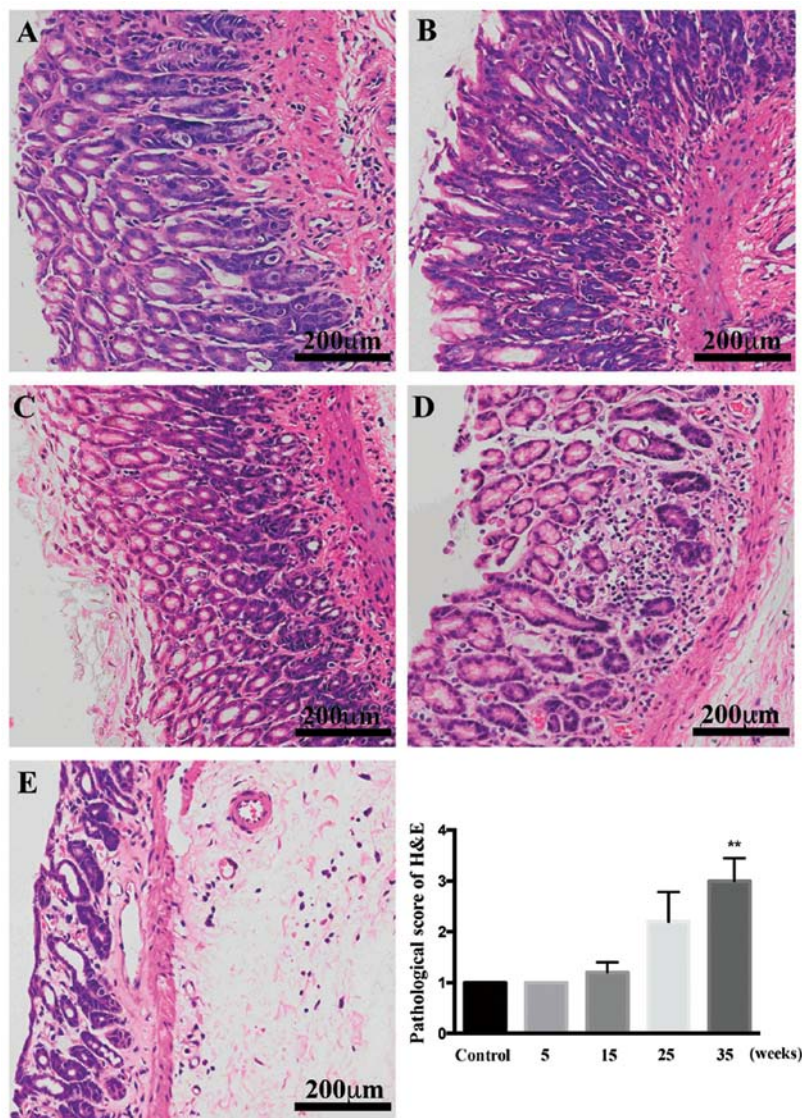


Figure 2. CAG is induced by intragastric administration of saturated NaCl and MNNG. Hematoxylin and eosin staining (magnification, x100) in (A) control group, (B) week 5, (C) week 15, (D) week 25, (E) week 35. Values are expressed as the mean \pm SEM (n=5/group). Data were analyzed using one-way analysis of variance (ANOVA). **P<0.01 vs. model group. CAG, chronic atrophic gastritis; MNNG, methyl-N¹-nitro-N-nitrosoguanidine.

of the stomach to cause DNA damage; thus, MNNG in the drinking water is used as a specific carcinogen to induce

GC (38). However, it takes a long time for MNNG in the drinking water to induce precancerous lesions in animals, and

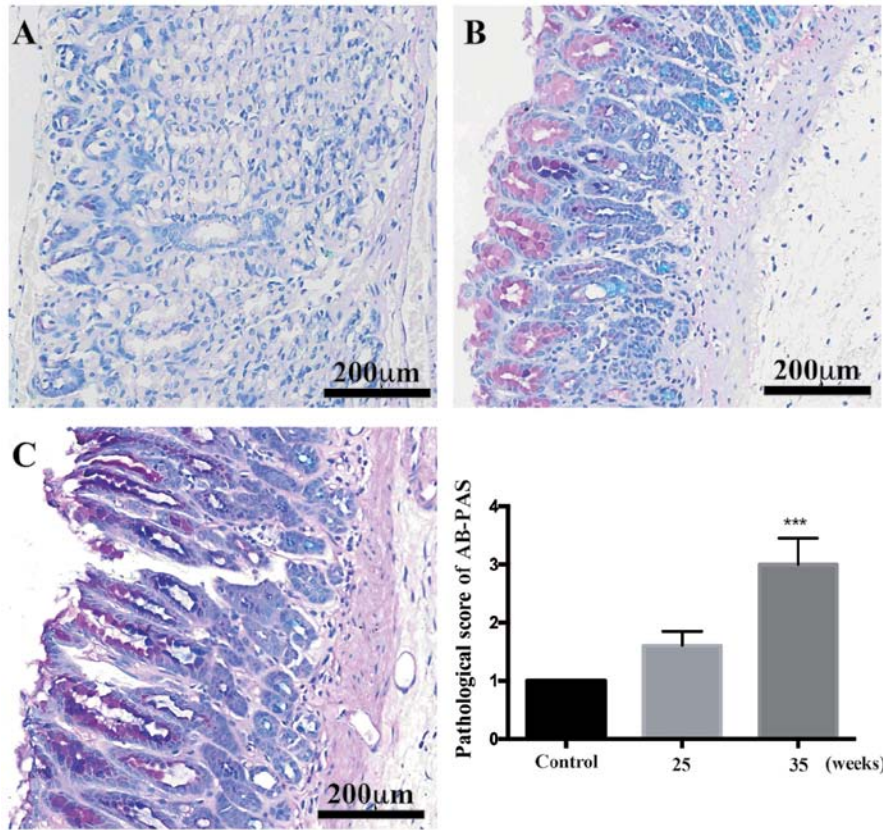


Figure 3. Gastric intestinal metaplasia is induced by intragastric administration of saturated NaCl and MNNG (Alcian blue-periodic acid-Schiff staining, x100 magnification). Gastric intestinal metaplasia changes were stained purple and blue. (A) Control group, (B) week 25, (C) week 35. Values are expressed as the mean \pm SEM (n=5/group). ***P<0.01 vs. model group.

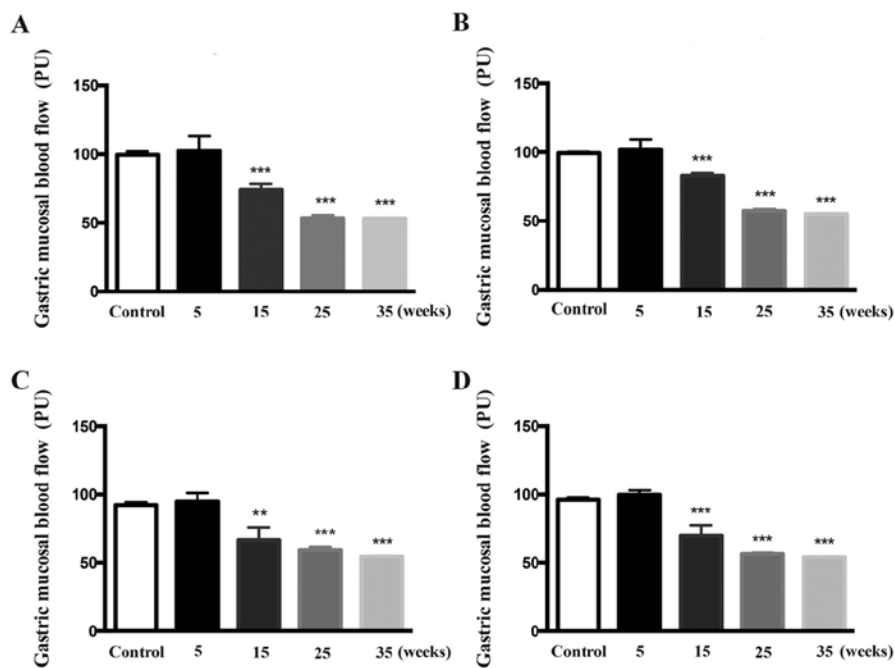


Figure 4. Gastric mucosal microcirculation disorder was induced by intragastrically administering saturated NaCl and MNNG. (A) GMBF of the fundus, (B) GMBF of the gastric body, (C) GMBF of the antrum, (D) GMBF of the whole stomach. Values are expressed as the mean \pm SEM (n=5/group). **P<0.01, ***P<0.001 vs. model group. GMBF, gastric mucosal blood flow.

the success rate is low (35). Thus, other stimulating factors, such as ammonia, sodium deoxycholate, salicylic acid and

ethanol, are also used to promote the development of CAG with precancerous lesions (Table II).

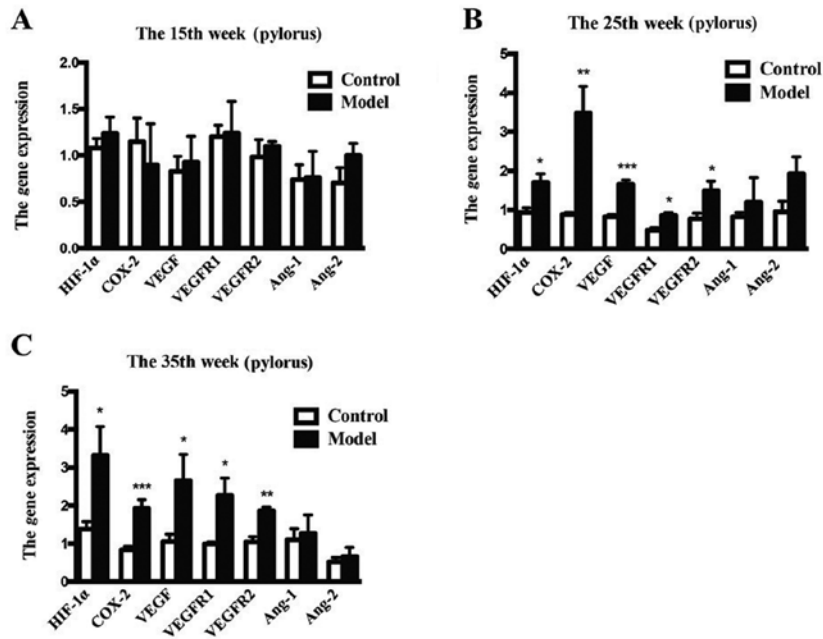


Figure 5. Gene expression levels of COX-2, HIF-1α, VEGFR1, VEGFR2, Ang-1 and Ang-2 in the gastric tissue. (A) Week 15, (B) week 25 and (C) week 35. Values are expressed as the mean ± SEM (n=5/group). *P<0.05, **P<0.01, ***P<0.001 vs. model group. COX-2, cyclooxygenase-2; HIF, hypoxia inducible factor; VEGFR, vascular endothelial growth factor receptor; Ang, angiotensin.

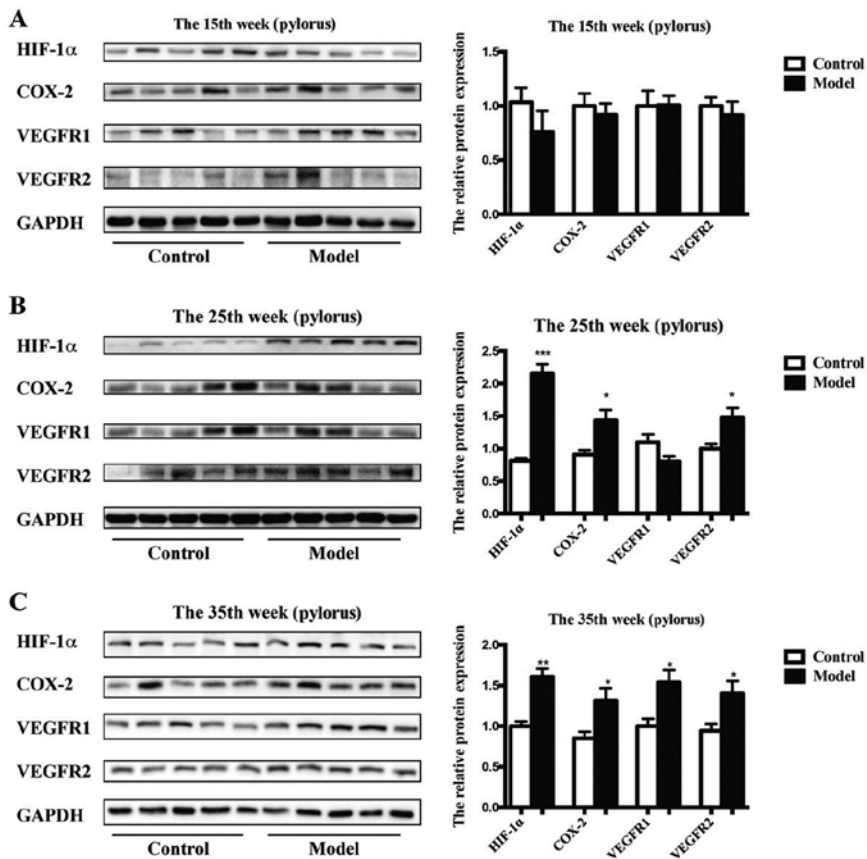


Figure 6. Protein expression levelsof COX-2, HIF-1α, VEGF and VEGFR1 in the gastric tissue. (A) Week 15, (B) week 25 and (C) week 35. Values were expressed as the mean ± SEM (n=5/group). *P<0.05, **P<0.01, ***P<0.001 vs. model group. COX-2, cyclooxygenase-2; HIF, hypoxia inducible factor; VEGFR, vascular endothelial growth factor receptor.

High-salt diets can directly damage the gastric mucosa and induce hypergastrinemia, leading to parietal cell loss and GC

progression (39). High-salt diets also promote inflammatory cell infiltration and increased COX-2 expression in Hp-infected

Table II. Methods of establishing chronic atrophic gastritis with precancerous lesions in rats.

Gastrogavage	Method					Time (week)	Mortality rate (%)	Success rate (%)	(Refs.)
	Water	Food	Operation	Others					
<i>H. pylori</i>	-	-	-	-	-	72	0	100	(29)
<i>H. pylori</i>	MNNG 20 m.m.p	-	-	-	-	50	0	60	(28)
-	-	-	Gastrojejunostomy	-	-	36	0	71.4	(31)
50-60 Paste containing 150 g/l NaCl, 2 ml	-	-	Spring pyloric implantation	-	-	16	0	100	(30)
-	MNNG 100 µg/ml	-	-	-	-	50	0	64.3	(35)
Sodium deoxycholate 20 mmol/l									
Ethanol 60%, 8 ml/kg									
Indomethacin 0.05%, 8 ml/kg	Ammonia 0.05-0.1%	-	-	-	-	42	0	100	(33)
MNNG 2 mM, 10 ml/kg									
Ethanol 5 ml/kg	-	-	-	-	-	32	0	100	(36)
MNNG 120 µg/ml, 10 ml/kg	Ammonia 0.1%	Ranitidine 0.03%	-	Fasting food Tail clamp	-	28	30	70	(32)
MNNG 120 µg/ml, 10 ml/kg									
Ethanol 35%, 3 ml/rat	Salicylic acid 2%	Ranitidine 0.03%	-	-	-	28	15.4	25	(37)
-	MNNG 100 µg/ml	NaCl 8%	-	-	-	42	45	31.3	(34)
MNNG, methyl-N'-nitro-N-nitrosoguanidine.									

Mongolian gerbils (40). Transgenic COX-2 expression and high-salt intake enhance susceptibility to methylnitrosourea (MNU)-induced GC development in mice (39,41). A 10% NaCl diet significantly increased the incidence of GC induced by oncogenic agents, such as MNNG, in drinking water (42). These findings indicate that high-salt intake plays an important role in GC progression. Reports on the induction of CAG with precancerous lesions in animals using MNNG and NaCl are rare. A previous study reported that combining 100 $\mu\text{g}/\text{ml}$ MNNG in the drinking water and chow pellets with 8% NaCl induced CAG with precancerous lesions in rats after modeling for 42 weeks. However, the mortality rate was 45% with only a 31.3% success rate (34).

Therefore, in the present study, only MNNG and saturated NaCl were intragastrically administered to induce CAG with IM in rats. At week 25, the success rate reached 60% with no deaths. At week 35, the success rate reached 100% with no deaths. Moreover, long-term saturated NaCl is similar to high-salt intake in clinical patients with CAG with IM (43,44). Therefore, the protocol described in the present study of inducing CAG with IM is simple, easy, controllable, less costly and repeatable.

Angiogenesis and microcirculatory disorders have been found in both CAG patients and animals (45,46). As a transcription factor, HIF-1 α directly regulates VEGF gene expression in cancer angiogenesis, especially under hypoxia (47). The HIF-1 α signaling pathway plays a vital role in blood microcirculatory disorders, including ischemia, hypoxia, inflammation and tumor angiogenesis (48-51). Gastric mucosal injury can induce upregulation of HIF-1 α , VEGF and COX-2 (52). COX-2 can enhance the expression of HIF-1 α and VEGF (53). HIF-1 α can also upregulate COX-2 expression in human endothelial cells (54). However, whether high-salt and MNNG intake can induce gastric microcirculatory disturbance and activation of the HIF-1 α pathway remains uncertain. In the present study, GMBF disturbance first appeared without significant activation of the HIF-1 α pathway at week 15. This demonstrated that blood microcirculatory problems began to appear before the development of HIF-1 α pathway dysfunction and CAG with IM, indicating that high-salt-induced gastric injury may be involved in blood microcirculatory disorders of the stomach. At week 25, CAG was successfully established, and the blood microcirculatory disorder was much more severe. The gastric mucosal blood flow was reduced, indicating that the decreased speed of the GMBF induced hypoxia in the model rats. HIF-1 α and COX-2 mRNA expression levels were significantly increased, indicating that blood microcirculatory disorder-induced hypoxia activated the HIF-1 α pathway and COX-2. After 35 weeks, moderate or severe atrophic gastritis with IM occurred in the model rats, indicating that high-salt-induced gastric mucosal injury may induce microcirculatory disorders, then microcirculatory disorder-induced hypoxia would induce abnormal HIF-1 α pathway expression and gastric inflammation evidenced by COX-2 upregulation. This would further enhance angiogenesis and consequently enhance the GC process (48,50,55,56). VEGFR1 and VEGFR2 are VEGF receptors (57). Upregulated VEGFR1 and VEGFR2 expressions in the gastric tissues of rats with CAG and IM are consistent with overactivation of the COX-2/HIF-1 α /VEGF pathway. In this study, blood microcirculatory disorders occurred during CAG with IM in rats. Thus,

this animal model can help clarify the molecular mechanisms of CAG with IM and help develop drugs to treat CAG with IM.

In conclusion, a new rat model of CAG with IM was stably and effectively established by intragastrically administering saturated NaCl and MNNG. Activation of the HIF-1 α pathways and gastric inflammation, resulted from high-salt-induced stomach microcirculatory disorders, might be involved in the pathological process of CAG with IM induced by high-salt and MNNG intake. However, the inconsistencies between replicate experiments is a limitation of the present study, which should be improved in future work.

Acknowledgements

Not applicable.

Funding

This work was supported by the National Natural Science Foundation of China (grant nos. 81403349, 81603354, 81673626), the Construction Project of Shanghai Union of Traditional Chinese Medicine [grant no. ZY(2018-2020)-FWTX-4018] and the Opening Project of Shanghai Key Laboratory of Compound Chinese Medicines (grant no. 17DZ2273300).

Availability of data and materials

The datasets used and/or analyzed during the current study are available from the corresponding author on reasonable request.

Authors' contributions

JYin and JYi performed experiments and drafted the manuscript. CY, BX and JL performed experiments. HH and XW made substantial contributions to conception and design, analysis and interpretation of data. HS and XF designed the research and revised the manuscript. All authors read and reviewed the final manuscript.

Ethics approval and consent to participate

All animal experiments were conducted according to the ethical guidelines of the National Guide for the Care and Use of Laboratory Animals and were approved by the Institutional Ethics Committee of Shanghai University of Traditional Chinese Medicine (approval no. SZY201703012).

Patient consent for publication

Not applicable.

Competing interests

The authors declare that they have no competing interests.

References

1. Bray F, Ferlay J, Soerjomataram I, Siegel RL, Torre LA and Jemal A: Global cancer statistics 2018: GLOBOCAN estimates of incidence and mortality worldwide for 36 cancers in 185 countries. *CA Cancer J Clin* 68: 394-424, 2018.

2. Forman D and Burley VJ: Gastric cancer: Global pattern of the disease and an overview of environmental risk factors. *Best Pract Res Clin Gastroenterol* 20: 633-649, 2006.
3. Cavatorta O, Scida S, Miraglia C, Barchi A, Nouvenne A, Leandro G, Meschi T, De' Angelis GL and Di Mario F: Epidemiology of gastric cancer and risk factors. *Acta Biomed* 89: 82-87, 2018.
4. Adamu MA, Weck MN, Gao L and Brenner H: Incidence of chronic atrophic gastritis: Systematic review and meta-analysis of follow-up studies. *Eur J Epidemiol* 25: 439-448, 2010.
5. Park YH and Kim N: Review of atrophic gastritis and intestinal metaplasia as a premalignant lesion of gastric cancer. *J Cancer Prev* 20: 25-40, 2015.
6. Zhao J, Zhao J, Du F, Zhang Y, Shen G, Zhu H, Ji F, Ma F, Dong L, Kan J, *et al*: Cardia and non-cardia gastric cancer have similar stage-for-stage prognoses after R0 resection: A large-scale, multicenter study in China. *J Gastrointest Surg* 20: 700-707, 2016.
7. Devesa SS, Blot WJ and Fraumeni JF Jr: Changing patterns in the incidence of esophageal and gastric carcinoma in the United States. *Cancer* 83: 2049-2053, 1998.
8. Powell J and McConkey CC: Increasing incidence of adenocarcinoma of the gastric cardia and adjacent sites. *Br J Cancer* 62: 440-443, 1990.
9. Cavaleiro-Pinto M, Peleteiro B, Lunet N and Barros H: *Helicobacter pylori* infection and gastric cardia cancer: Systematic review and meta-analysis. *Cancer Causes Control*. Netherlands 22: 375-387, 2011.
10. Yoon H and Kim N: Diagnosis and management of high risk group for gastric cancer. *Gut Liver* 9: 5-17, 2015.
11. Hipgrave DB, Chang S, Li X and Wu Y: Salt and sodium intake in China. *JAMA* 315: 703-705, 2016.
12. Bergin IL, Sheppard BJ and Fox JG: *Helicobacter pylori* infection and high dietary salt independently induce atrophic gastritis and intestinal metaplasia in commercially available outbred Mongolian gerbils. *Dig Dis Sci* 48: 475-485, 2003.
13. D'Elia L, Rossi G, Ippolito R, Cappuccio FP and Strazzullo P: Habitual salt intake and risk of gastric cancer: A meta-analysis of prospective studies. *Clin Nutr* 31: 489-498, 2012.
14. Song JH, Kim YS, Heo NJ, Lim JH, Yang SY, Chung GE and Kim JS: High salt intake is associated with atrophic gastritis with intestinal metaplasia. *Cancer Epidemiol Biomarkers Prev* 26: 1133-1138, 2017.
15. Montani A, Sasazuki S, Inoue M, Higuchi K, Arakawa T and Tsugane S: Food/nutrient intake and risk of atrophic gastritis among the *Helicobacter pylori*-infected population of north-eastern Japan. *Cancer Sci* 94: 372-377, 2003.
16. Wiseman M: The second World Cancer Research Fund/American Institute for Cancer Research expert report. Food, nutrition, physical activity, and the prevention of cancer: A global perspective. *Proc Nutr Soc* 67: 253-256, 2008.
17. Kim J, Park S and Nam BH: Gastric cancer and salt preference: A population-based cohort study in Korea. *Am J Clin Nutr* 91: 1289-1293, 2010.
18. Ling L, Tao H, Lu L, Qianqian S and Mingyu S: Summary and review of animal models for chronic atrophic gastritis and precancerous lesions of gastric cancer. *Chinese J Exp Trad Med Formulae* 24: 1-8, 2018.
19. Fuhua L, Xiaoguang Q, Junhua L and Mei L: Research progress on animal models of chronic atrophic gastritis. *Chinese Med Moedern distance Educ China* 16: 18-19, 2018.
20. Li Y, Xia R, Zhang B and Li C: Chronic atrophic gastritis: A review. *J Environ Pathol Toxicol Oncol* 37: 241-259, 2018.
21. Sipponen P and Maaroos HI: Chronic gastritis. *Scand J Gastroenterol* 50: 657-667, 2015.
22. Lee JY, Kim N, Nam RH, Choi YJ, Seo JH, Lee HS, Oh JC and Lee DH: No correlation of inflammation with colonization of *Helicobacter pylori* in the stomach of mice fed high-salt diet. *J Cancer Prev* 19: 144-151, 2014.
23. Toyoda T, Tsukamoto T, Yamamoto M, Ban H, Saito N, Takasu S, Shi L, Saito A, Ito S, Yamamura Y, *et al*: Gene expression analysis of a *Helicobacter pylori*-infected and high-salt diet-treated mouse gastric tumor model: Identification of CD177 as a novel prognostic factor in patients with gastric cancer. *BMC Gastroenterol* 13: 122, 2013.
24. Amara S, Alotaibi D and Tiriveedhi V: NFAT5/STAT3 interaction mediates synergism of high salt with IL-17 towards induction of VEGF-A expression in breast cancer cells. *Oncol Lett* 12: 933-943, 2016.
25. Amara S and Tiriveedhi V: Inflammatory role of high salt level in tumor microenvironment (Review). *Int J Oncol* 50: 1477-1481, 2017.
26. Zhang Y, Li J, Zhu L and Cui W: Effect of three methods for activating blood circulation on early stage apoptosis in rats with chronic atrophic gastric complicated precancerous lesion. *Chinese J Integr Tradit West Med* 28: 448-450, 2008.
27. Livak KJ and Schmittgen TD: Analysis of relative gene expression data using real-time quantitative PCR and the 2(-Delta Delta C(T)) method. *Methods* 25: 402-408, 2001.
28. Shimizu N, Inada KI, Tsukamoto T, Nakanishi H, Ikehara Y, Yoshikawa A, Kaminishi M, Kuramoto S and Tatematsu M: New animal model of glandular stomach carcinogenesis in Mongolian gerbils infected with *Helicobacter pylori* and treated with a chemical carcinogen. *J Gastroenterol* 34: 61-66, 1999.
29. Honda S, Fujioka T, Tokieda M, Satoh R, Nishizono A and Nasu M: Development of *Helicobacter pylori*-induced gastric carcinoma in mongolian gerbils. *Cancer Res* 58: 4255-4259, 1998.
30. Shi XY, Zhao FZ, Dai X, Ma LS, Dong XY and Fang J: Effect of jianpiyiwei capsule on gastric precancerous lesions in rats. *World J Gastroenterol* 8: 608-612, 2002.
31. Dong Xi, Lei D, Jun G, Ningli C, Huibin Q and Jinyan L: Experimental study on the relationship between cell proliferation and apoptosis and the expression of the related gene in rats with duodenogastric reflux. *J Xi'an Jiaotong Univ Sci* 25: 261-265, 2004.
32. Wei Y, Yang J, Yang H and Song Y: Experimental effect of Yiqi Huayu Jiedu principle on chronic atrophic gastritis with dysplasia rats. *Chinese J Gastroenterol Hepatol* 20: 916-919, 2011.
33. Si J, Zhou W, Wu J, Cao Q, Xiang Z, Jiang L, Lü W and Huang H: Establishment of an animal model of chronic atrophic gastritis and a study on the factors inducing atrophy. *Chin Med J (Engl)* 114: 1323-1325, 2001.
34. Gu J, Hu X, Shao W, Ji T, Yang W, Zhuo H, Jin Z, Huang H, Chen J, Huang C and Lin D: Metabolomic analysis reveals altered metabolic pathways in a rat model of gastric carcinogenesis. *Oncotarget* 7: 60053-60073, 2016.
35. Tsukamoto H, Mizoshita T, Katano T, Hayashi N, Ozeki K, Ebi M, Shimura T, Mori Y, Tanida S, Kataoka H, *et al*: Preventive effect of rebamipide on N-methyl-N'-nitro-N-nitrosoguanidine-induced gastric carcinogenesis in rats. *Exp Toxicol Pathol* 67: 271-277, 2015.
36. Xu J, Shen W, Pei B, Wang X, Sun D, Li Y, Xiu L, Liu X, Lu Y, Zhang X and Yue X: Xiao Tan He Wei Decoction reverses MNNG-induced precancerous lesions of gastric carcinoma in vivo and vitro: Regulation of apoptosis through NF- κ B pathway. *Biomed Pharmacother* 108: 95-102, 2018.
37. Ren J, Yang Y, Qu X, Ying L, Yang M and Yan N: Evaluation of a compound modling method with N-methyl-N'-nitro-N-nitrosoguanidine for establishing chronic atrophic gastritis model rats. *J Tradit Chinese Med* 58: 1961-1964, 2017.
38. Tsukamoto T, Mizoshita T and Tatematsu AM: Animal models of stomach carcinogenesis. *Toxicol Pathol* 35: 636-648, 2007.
39. Wang XQ, Terry PD and Yan H: Review of salt consumption and stomach cancer risk: Epidemiological and biological evidence. *World J Gastroenterol* 15: 2204-2213, 2009.
40. Kato S, Matsukura N, Matsuda N, Yamashita N, Naito Z and Tajiri T: How to evaluate mRNA gene expressions of cancer related cytokines for the infectious diseases including stomach and liver carcinogenesis and prevention. *Cancer Res* 66: 871, 2006.
41. Leung WK, Wu K, Wong CYP, Cheng AS, Ching AK, Chan AW, Chong WW, Go MY, Yu J, To KF, *et al*: Transgenic cyclooxygenase-2 expression and high salt enhanced susceptibility to chemical-induced gastric cancer development in mice. *Carcinogenesis* 29: 1648-1654, 2008.
42. Takahashi M and Hasegawa R: Enhancing effects of dietary salt on both initiation and promotion stages of rat gastric carcinogenesis. *Princess Takamatsu Symp* 16: 169-182, 1985.
43. Chen Z, Li K, Bi J and Wang B: Sodium intake, salt taste and gastric cancer risk according to *Helicobacter pylori* infection, smoking, histological type and tumor site in China. *Asian Pacific J Cancer Prev* 13: 2481-2484, 2012.
44. You W, Blot WJ, Chang YS, Ershow AG, Yang Z, An Q, Henderson B, Xu GW, Fraumeni JF Jr and Wang TG: Diet and high risk of stomach cancer in shandong, China. *Cancer Res* 48: 3518-3523, 1988.
45. Yu S, E Z and Liu S: Examination of the gastric mucosal vessels in chronic gastritis by color Doppler flow imaging. *Chinese J Ultrasound Med* 17: 45-46, 2001.
46. Pousa ID and Gisbert JP: Gastric angiogenesis and *Helicobacter pylori* infection. *Rev Esp Enferm Dig* 98: 527-541, 2006 (In English, Spanish).

47. Mirzoeva S, Kim ND, Chiu K, Franzen CA, Bergan RC and Pelling JC: Inhibition of HIF-1 alpha and VEGF expression by the chemopreventive bioflavonoid apigenin is accompanied by Akt inhibition in human prostate carcinoma PC3-M cells. *Mol Carcinog* 47: 686-700, 2008.
48. Huang SP, Wu MS, Shun CT, Wang HP, Hsieh CY, Kuo ML and Lin JT: Cyclooxygenase-2 increases hypoxia-inducible factor-1 and vascular endothelial growth factor to promote angiogenesis in gastric carcinoma. *J Biomed Sci* 12: 229-241, 2005.
49. Stoeltzing O, Liu W, Reinmuth N, Fan F, Parikh AA, Bucana CD, Evans DB, Semenza GL and Ellis LM: Regulation of hypoxia-inducible factor-1alpha, vascular endothelial growth factor, and angiogenesis by an insulin-like growth factor-I receptor autocrine loop in human pancreatic cancer. *Am J Pathol* 163: 1001-1011, 2003.
50. Liu LZ, Jing Y, Jiang LL, Jiang XE, Jiang Y, Rojanasakul Y and Jiang BH: Acacetin inhibits VEGF expression, tumor angiogenesis and growth through AKT/HIF-1 α pathway. *Biochem Biophys Res Commun* 413: 299-305, 2011.
51. Park SA, Jeong MS, Ha KT and Jang SB: Structure and function of vascular endothelial growth factor and its receptor system. *BMB Rep* 51: 73-78, 2018.
52. Liu D, He Q and Liu C: Correlations among *Helicobacter pylori* infection and the expression of cyclooxygenase-2 and vascular endothelial growth factor in gastric mucosa with intestinal metaplasia or dysplasia. *J Gastroenterol Hepatol* 25: 795-799, 2010.
53. Hu H, Zheng H and Lu X: Effects of 'Weiqiyin Drink' in reversing chronic atrophic gastritis complicated with precancerous morbid cells. *Chinese J Integr Tradit West Med Gastro-spleen* 9: 32-34, 2001.
54. Naomoto Y, Gunduz M, Takaoka M, Okawa T, Gunduz E, Nobuhisa T, Kobayashi M, Shirakawa Y, Yamatsuji T, Sonoda R, *et al*: Heparanase promotes angiogenesis through Cox-2 and HIF1alpha. *Med Hypotheses* 68: 162-165, 2007.
55. Tarnawski AS, Ahluwalia A and Jones MK: Angiogenesis in gastric mucosa: An important component of gastric erosion and ulcer healing and its impairment in aging. *J Gastroenterol Hepatol* 29 (Suppl 4): S112-S123, 2014.
56. Isobe T, Aoyagi K, Koufujii K, Shirouzu K, Kawahara A, Taira T and Kage M: Clinicopathological significance of hypoxia-inducible factor-1 alpha (HIF-1 α) expression in gastric cancer. *Int J Clin Oncol* 18: 293-304, 2013.
57. Kopparapu PK, Boorjian SA, Robinson BD, Downes M, Gudas LJ, Mongan NP and Persson JL: Expression of VEGF and its receptors VEGFR1/VEGFR2 is associated with invasiveness of bladder cancer. *Anticancer Res* 33: 2381-2390, 2013.



This work is licensed under a Creative Commons Attribution-NonCommercial-NoDerivatives 4.0 International (CC BY-NC-ND 4.0) License.